Supplementary Information (SI) for Journal of Materials Chemistry C.

Supporting Information

Self-Powered, Low-Dark-Current, High-Detectivity $CsPbBr_3$ Nanowire Photodetectors with Excellent Weak-Light Detection Ability

Boao Xiao,[1, 3, #] Shuiguo Wen,[2, #] Jianqiang Zhang,[1, #] Zheng Gao,[1, #] Yapeng Tang,[1] Dingjun Wu,[1, *] Jiang Zhao,[3, *] Hai Zhou[1, *]

[1]International School of Microelectronics, Dongguan University of Technology, Dongguan, 523808, PR China.

[2]Engineering Training Center, Guilin University of Aerospace Technology, Guilin, 541004, PR China.

[3]School of Microelectronics, Hubei University, Wuhan, 430062, PR China.

[#] These authors contribute equally

* Corresponding authors: E-mail: 1309622641@qq.com (Dingjun Wu), zhaojiang@hubu.edu.cn (Jiang Zhao), hizhou@dgut.edu.cn (Hai Zhou)

S1 Materials

DMF (Macklin, 99.9%); Lead iodide (PbI_2, Boerid, 99.999%); Cesium iodide (CsI, Macklin, 99.9%); Cesium Bromide (CsBr, Aladdin, 99.9%); Anhydrous methanol (Macklin, 98%); Isopropanol (Macklin, 99.9%); 1-octyl-3-methylimidazolium hydrogen sulfate ($OMIMHSO_4$, Macklin, 98%).

S2 Device Fabrication

ITO glass substrates are sequentially ultrasonically cleaned with detergent, deionized water, isopropanol, and alcohol for 20 minutes. Following this, a SnO_2 solution (1 mL) is diluted in deionized water (4 mL), and the cleaned substrates are treated in an ultraviolet ozone cleaner for 30 minutes. Subsequently, 100 μL of the SnO_2 solution is spin-coated onto the substrates at 4000 rpm for 30 seconds, followed by annealing at 150°C for 30 minutes to form the SnO_2 thin film. The substrates undergo additional treatment in the ultraviolet ozone cleaner for 50 minutes. Then, the substrates are preheated at 70°C for 5 minutes and coated with 90 μL of a $PbI_2/OMIMHSO_4$ solution in DMF (1 mol mL^{-1}, with varying $OMIMHSO_4$ concentrations: 0, 5, 7.5, 10, 12.5 mg mL^{-1}) at 3000 rpm for 30 seconds, followed by annealing at 70°C for 15 minutes to form the PbI_2 film. The PbI_2 film is then immersed in a petri dish containing 30 mL of CsI (8 mg mL^{-1}) in methanol for 15 hours, rinsed with isopropanol, and spun dry at 2000 rpm for 20 seconds to obtain the non-perovskite phase $CsPbI_3$ nanowire film. This film is further immersed in 30 mL of CsBr (8 mg mL^{-1}) in methanol for 4 hours, rinsed with isopropanol, and spun dry at 2000 rpm for 20 seconds. Then, the substrate is annealed at 200°C for 15 minutes to obtain the perovskite phase $CsPbBr_3$ nanowire film. Finally, the carbon electrodes were deposited on the surface of the $CsPbBr_3$ nanowire film by scraping coating and subsequently annealed at 100°C for 20 minutes to complete the device fabrication. The effective area of the device is 0.04 cm^2.

S3 Characterizations

Scanning Electron Microscope (SEM) images of the $CsPbBr_3$ nanowire films were obtained using a VeriosG4UC SEM. X-ray Diffraction (XRD) patterns were recorded using a desktop X-ray diffractometer (MINIFLEX600). Photoluminescence spectra were acquired with a steady-state and time-resolved fluorescence spectrophotometer (FLS-1000). Ultraviolet-visible-near-infrared (UV-Vis-NIR) absorption spectra were measured using a UV-Vis-NIR spectrophotometer (CARY5000).

S4 Device Measurements

Current-voltage (I-V) and current-time (I-t) characteristics were measured using a Keithley 2450 SourceMeter. A 405 nm laser was employed as the light source, and its intensity was modulated through a series of neutral density filters, with the intensity measured by a standard Si detector. All measurements were conducted in air.

S5 Supplementary Figures and Tables

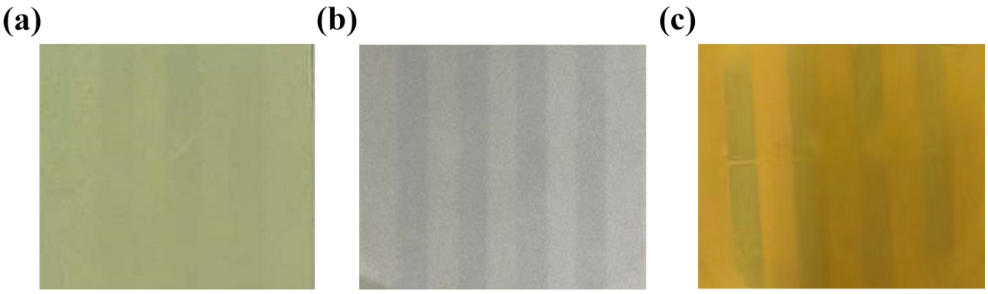

Figure S1. (a) N-$CsPbI_3$ NWs film. (b) N-$CsPbBr_3$ NWs film. (c) P-$CsPbBr_3$ NWs film.

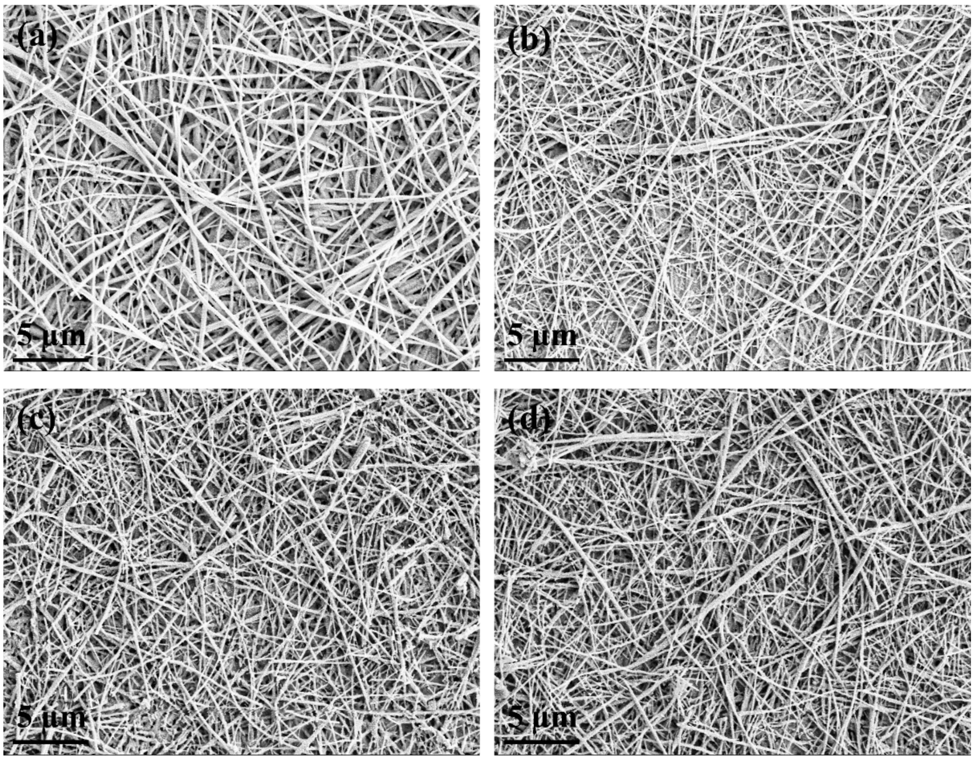

Figure S2. SEM images of nanowire films with different concentrations of $OMIMHSO_4$: (a) 0 mg mL^{-1}, (b) 5 mg mL^{-1}, (c) 10 mg mL^{-1}, (d) 12.5 mg mL^{-1}.

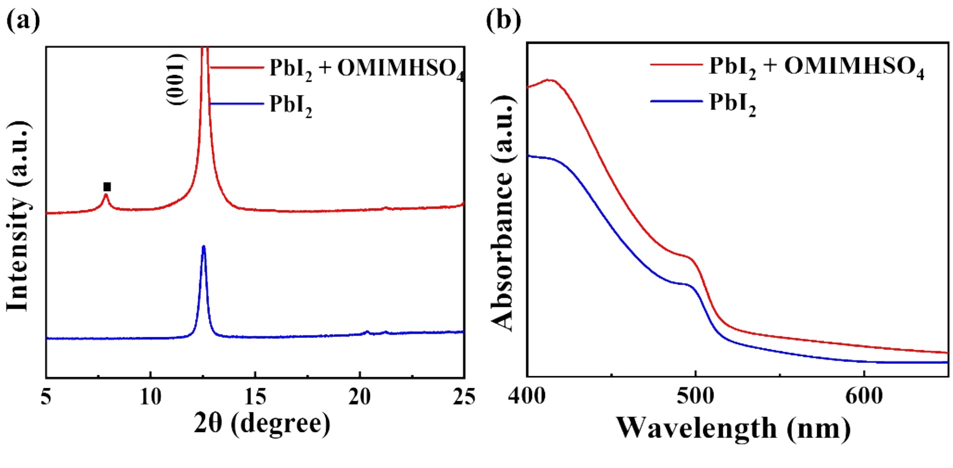

Figure S3. (a) XRD patterns and (b) optical absorption spectra of PbI_2 and PbI_2-$OMIMHSO_4$ films.

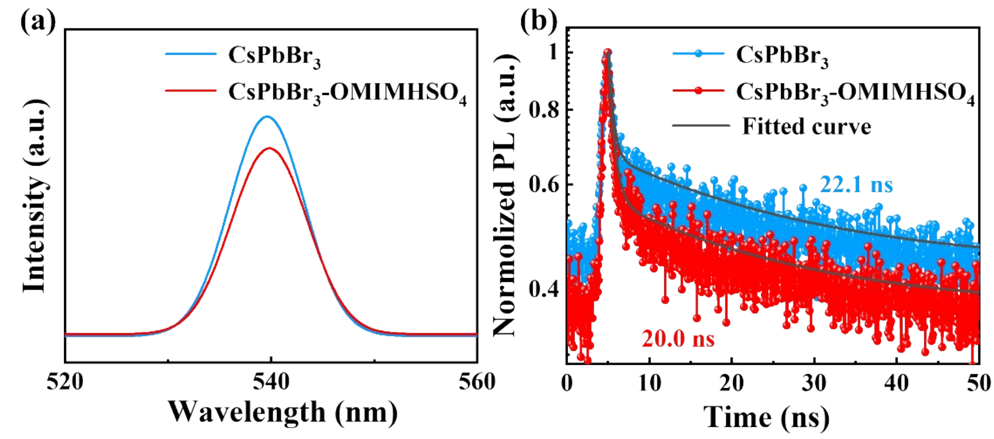

Figure S4. (a) Photoluminescence (PL) spectra and (b) time-resolved photoluminescence (TRPL) spectra of $CsPbBr_3$ and $CsPbBr_3$-$OMIMHSO_4$ nanowire films deposited on ITO.

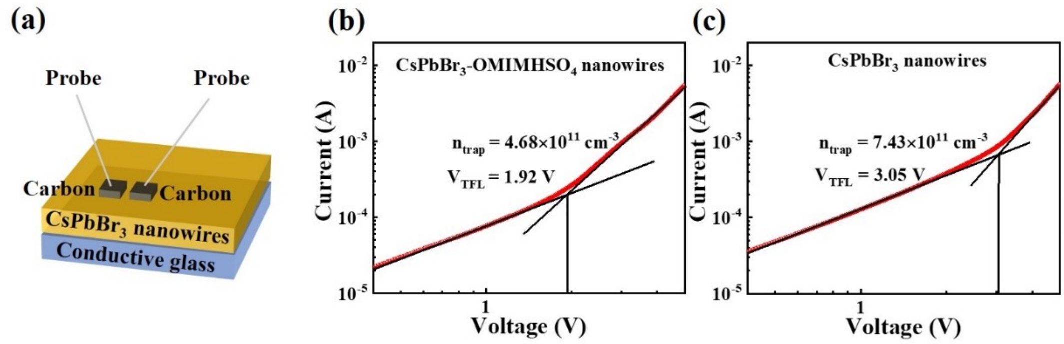

Figure S5. (a) Schematic diagram of the space-charge-limited current (SCLC) test setup. (b) SCLC characteristics of the $CsPbBr_3$ nanowire photodetector with 7.5 mg mL^{-1} $OMIMHSO_4$. (c) SCLC characteristics of the $CsPbBr_3$ nanowire photodetector without $OMIMHSO_4$.

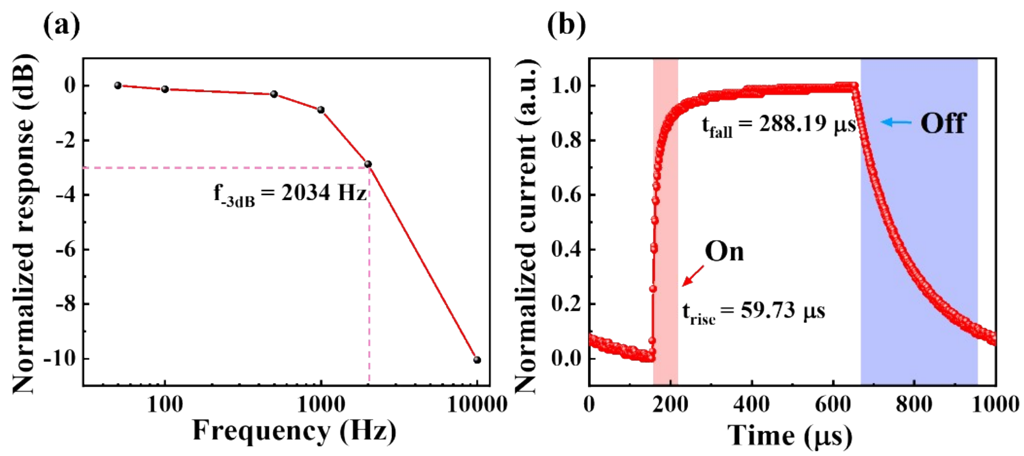

Figure S6. Photodetector without $OMIMHSO_4$: (a) f_{-3dB}, (b) Response time.

Table S1. The calibration data for the laser power density using a standard Si detector.

Responsivity (A/W)	Light current (A)	Dark current (A)	Si detector area (mm^2)	Power (W)	Power density (mW/cm^2)
0.28	2.689×10^{-2}	1.45×10^{-10}		9.6×10^{-2}	6.67×10^{3}
0.28	2.077×10^{-3}	1.59×10^{-11}		7.42×10^{-3}	5.15×10^{2}
0.28	1.05×10^{-4}	5.76×10^{-12}		3.75×10^{-4}	2.60×10^{1}
0.28	5.62×10^{-6}	2.41×10^{-12}		2.01×10^{-5}	1.39×10^{0}
0.28	4.26×10^{-7}	2.09×10^{-12}		1.52×10^{-6}	1.06×10^{-1}
0.28	3.49×10^{-8}	2.49×10^{-12}	1.44	1.25×10^{-7}	8.66×10^{-3}
0.28	1.20×10^{-9}	2.00×10^{-12}		4.28×10^{-9}	2.97×10^{-4}
0.28	7.53×10^{-11}	1.49×10^{-12}		2.64×10^{-10}	1.83×10^{-5}
0.28	9.96×10^{-12}	1.34×10^{-12}		3.08×10^{-11}	2.14×10^{-6}
0.28	1.605×10^{-12}	1.12×10^{-12}		1.64×10^{-12}	1.14×10^{-7}

Table S2. The device area, light current, dark current, photocurrent, laser power density, and calculated responsivity and detectivity.

Device area (cm^2)	Light current (A)	Dark current (A)	Photocurrent (A)	Laser power density (mW cm^{-2})	Calculated responsivity (A/W)	Calculated detectivity (Jones)
0.04	9.92×10^{-4}	3.73×10^{-9}	9.92×10^{-4}	6.67×10^{3}	3.72×10^{-3}	2.15×10^{10}
	1.36×10^{-4}	1.87×10^{-9}	1.36×10^{-4}	5.15×10^{2}	6.60×10^{-3}	5.40×10^{10}
	7.33×10^{-6}	8.27×10^{-10}	7.33×10^{-6}	2.60×10^{1}	7.04×10^{-3}	8.65×10^{10}
	6.71×10^{-7}	3.68×10^{-10}	6.71×10^{-7}	1.39×10^{0}	1.20×10^{-2}	2.22×10^{11}
	4.78×10^{-8}	9.27×10^{-11}	4.77×10^{-8}	1.06×10^{-1}	1.13×10^{-2}	4.15×10^{11}
	3.57×10^{-9}	2.24×10^{-11}	3.55×10^{-9}	8.66×10^{-3}	1.02×10^{-2}	7.65×10^{11}
	1.70×10^{-10}	4.59×10^{-12}	1.65×10^{-10}	2.97×10^{-4}	1.39×10^{-2}	2.30×10^{12}
	8.52×10^{-11}	3.68×10^{-12}	8.15×10^{-11}	1.83×10^{-5}	1.11×10^{-1}	2.05×10^{13}
	1.32×10^{-11}	3.68×10^{-12}	9.52×10^{-12}	2.14×10^{-6}	1.11×10^{-1}	2.05×10^{13}
	5.43×10^{-12}	3.68×10^{-12}	1.75×10^{-12}	1.14×10^{-7}	3.85×10^{-1}	7.09×10^{13}

Table S3. Performance comparison of perovskite nanowire-based photodetectors.

Detector Type	Responsivity ($A W^{-1}$)	Detectivity (Jones)	LDR (dB)	Response Time	Refs.
$MAPbX_3$ NWs	0.23	7.1×10^{11}	--	53.2/50.2 μs	[1]
$MAPb(I_{1-x}Br_x)_3$ NWs	1.25×10^4	1.73×10^{11}	150	0.34/0.42 μs	[2]
$MAPbI_3$ NWs	460	2.6×10^{13}	--	180/330 μs	[3]
$MAPbI_3$ NWs	1.32	2.5×10^{12}	--	0.2/0.3 μs	[4]
$(MTEA)_2(MA)_{n-1}Pb_nI_{3n+1}$ NWs	7.3×10^3	3.9×10^{15}	--	40/52.2 μs	[5]
$MAPbI_3$ NWs	37.14	2.06×10^{13}	160	91/563 μs	[6]
$CsPb_xSn_{1-x}(Br_yI_{1-y})_3$ NWs	8.5×10^{-3}	2×10^{10}	120	4.25/4.82 ms	[7]
$CsSnI_3$ NWs	9.9×10^{-3}	7.2×10^8	73	446/534 ms	[8]
$CsPbBr_3$ NWs	0.3	1×10^{13}	135	0.4/0.43 ms	[9]
$CsPbBr_3$ NWs	4.4×10^3	--	--	252/300 μs	[10]
$CsPbBr_3$ NWs	0.385	7.09×10^{13}	215	45.14/204.52 μs	This work

1 I. M. Asuo, D. Gedamua, I. Kaa, L. F. Gerleina, F. X. Fortiera, A. Pignoletb, S. G. Cloutiera and R. Nechachea, *Nano Energy*, 2018, **51**, 324-332.

2 W. Deng, L. M. Huang, X. Z. Xu, X. J. Zhang, X. C. Jin, S. T. Lee and J. S. Jie, *Nano Lett.*, 2017, **17**, 2482-2489.

3 X. Z. Xu, X. J. Zhang, W. Deng, L. M. Huang, W. Wang, J. S. Jie and X. H. Zhang, *ACS Appl. Mater. Interfaces*, 2018, **10**, 10287-10295.

4 H. Deng, D. D. Dong, K. K. Qiao, L. L. Bu, B. Li, D. Yang, H. E. Wang, Y. B. Cheng, Z. X. Zhao, J. Tang and H. S. Song, *Nanoscale*, 2015, **7**, 4163-4170.

5 M. Yuan, Y. J. Zhao, J. G. Feng, H. F. Gao, J. J. Zhao, L. Jiang and Y. C. Wu, *ACS*

Appl. Mater. Interfaces, 2022, **14**, 1601-1608.

6 D. J. Wu, Y. C. Xu, H. Zhou, X. Feng, J. Q. Zhang, X. Y. Pan, Z. Gao, R. Wang, G. K. Ma, L. Tao, H. B. Wang, J. X. Duan, H. Z. Wan, J. Zhang, L. P. Shen, H. Wang and T. Y. Zhai, *InfoMat*, 2022, **4**, e12320.

7 X. M. Tang, H. Zhou, X. Y. Pan, R. H. Liu, D. J. Wu and H. Wang, *ACS Appl. Mater. Interfaces*, 2020, **12**, 4843-4848.

8 H. Zhou, X. M. Tang and Z. Gao, *Colloid Interface Sci. Commun.*, 2022, **49**, 100638.

9 H. Zhou, Z. N. Song, C. R. Grice, C. Chen, J. Zhang, Y. F. Zhu, R. H. Liu, H. Wang and Y. F. Yan, *Nano Energy*, 2018, **53**, 880-886.

10 M. Shoaib, X. H. Zhang, X. X. Wang, H. Zhou, T. Xu, X. Wang, X. L. Hu, H. W. Liu, X. P. Fan, W. H. Zheng, T. F. Yang, S. Z. Yang, Q. L. Zhang, X. L. Zhu, L. T. Sun and A. L. Pan, *J. Am. Chem. Soc.*, 2017, **139**, 15592-15595.